Technical Paper

FEM modeling for predicting temperature profile of heat affected zone in single spark EDM process

S. C. Sonthalia*, Gaurav Bartarya, S. Mullick

Indian Institute of Technology Bhubaneswar, Khordha, India

Presented in International Conference on Precision, Micro, Meso and Nano Engineering (COPEN - 12: 2022)
December 8 - 10, 2022 IIT Kanpur, India

ABSTRACT

Existing single spark models are far from accurate since they are based on simplified considerations like constant plasma radius, constant material characteristics, and constant surface temperature during actual discharge application. This work depicts a simulation study of a single spark during EDM using finite element method while taking into account the important factors like temperature dependence of material characteristics, plasma channel radius variations with current, and discharge duration. This model offers a more realistic temperature distribution profile in the workpiece. FEM simulation shows that increasing pulse on-time results in a greater depth of heat-affected zone, and increasing pulse current results in a modest decrease in heat-affected zone depth due to variation in spark radius.

KEYWORDS

Single Spark Analysis,
Electrical Discharge Machining,
Heat Affected Zone,
Finite Element Model.

1. Introduction

Material removal uses the thermal energy generated by spark discharges in the widely used non-traditional machining technique known as electrical discharge machining (EDM). The spark gap refers to the tiny space between the workpiece (cathode) and tool (anode) that is between 10 and 100 microns in size. A liquid dielectric is present inside the spark gap. Initially acting as an insulator, this liquid dielectric undergoes breakdown to generate a plasma channel made up of positive ions and electrons given the right electrical circumstances. The applied electric field speeds up these ions and electrons as they strike the electrodes at high speeds. This causes very small sections on both cathodic and anodic surfaces to be localized and heated to extremely high temperatures, which causes material loss through melting and evaporation.

On the electrode surfaces, the remaining molten material re-solidifies to create a recast layer since the dielectric is unable to flush it away completely. In both electrodes, the temperature gradient also causes a heat-affected zone (HAZ) beneath the recast layer. Because anodes release positive ions rather than electrons, they have a larger plasma channel radius than cathodes. Due to the reduced heat flow intensity, anodic craters are smaller than cathodic craters in size.

The formation of plasma, heat conduction, heat convection, heat radiation, plasma channel implosion, shock wave generation, dielectric removal of molten metal, re-solidification, and electrical phenomena, chemical phenomena, etc., are just a few of the many diverse phenomena that occur during every spark discharge, along with their interactions. The spark generation and material removal mechanisms still need to be further understood and clarified because of these complicated underlying phenomena (Schumacher, 2004).

A cathode erosion model DiBitonto et al. (1989) was provided to forecast the crater size when the operational parameters are known. This is the most notable work among the analytical models. A single spark discharge was simulated by the researchers (Yadav et al., 2002). Thermal strains and the temperature distribution brought on by the input heat flux during a spark discharge on the work material was estimated. A thin layer was observed to be formed surrounding the discharge location with substantial levels of compressive and tensile stresses, which could cause damage to the work surface. Researchers (Joshi & Pande, 2010) have observed that the prediction of crater size and

*Corresponding author E-mail: scs11@iitbbs.ac.in

https://doi.org/10.58368/MTT.22.5.2023.56-62

MRR is improved by using realistic assumptions in form of temperature dependence of material properties and incorporation of latent heat of fusion during FE simulation. In another work Kalajahi et al. (2013) finite element approach was used to examine the impact of various operating factors on the temperature distribution on the cathode. As operating parameters like current, voltage and duty cycle increased, so did the temperature distribution and, consequently, the size of the craters. However, crater size's importance increases to a large discharge duration value. The crater size decreases as discharge time is increased more.

Proper temperature profile prediction is required for crater shape prediction and consequently for surface texture prediction in various spark conditions and operational environments. Therefore, the current work's objective is to create a FE model that predicts the temperature profile obtained during a single discharge of the EDM process while taking into account the crucial factors discussed above.

2. Finite Element Model

The model takes into account crucial process variables like temperature-dependent material properties, a variable plasma channel radius, cathode energy fraction, and plasma flushing efficiency in order to make a more accurate prediction of temperature profile.

The heat transfer equation without internal heat generation term is commonly used for thermal modelling to describe the heat distribution during each discharge. Since it is believed that the heat produced by a single spark that transfers to the workpiece is axisymmetric, the heat transfer equation in cylindrical coordinates is given as below-

$$\frac{\partial T}{\partial t} = \alpha\left(\frac{\partial^2 T}{\partial x^2} + \frac{\partial^2 T}{\partial y^2}\right) \quad \text{.....(1)}$$

$$\alpha = \frac{K}{\rho C_p} \quad \text{.....(2)}$$

Where T is temperature, K is thermal conductivity, ρ is average material density, C_p average specific heat capacity and x and y are coordinate axis.

The area of the workpiece around the spark when heat flux is delivered to surface 1 (Fig. 1) is considered to be a small cylindrical area.

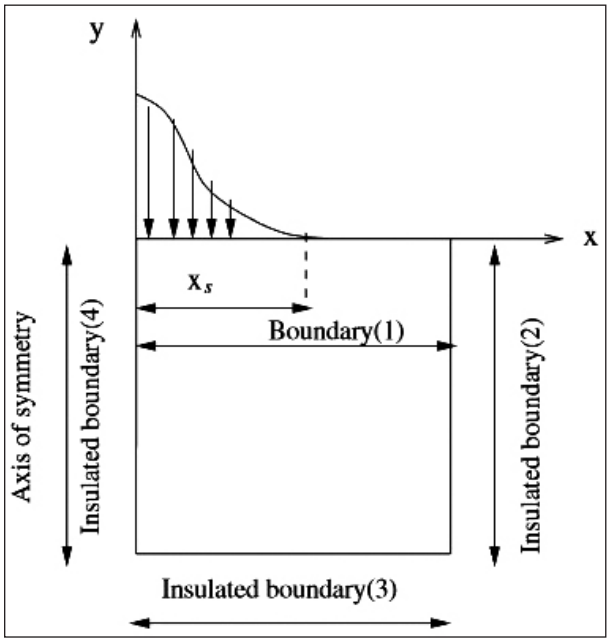

Fig. 1. Thermal model of EDM process.

Conventional heat transfer occurs on the remainder of region 1 as a result of the cooling impact of the dielectric fluid. Spark region is quite far from boundaries 2 and 3, and spark very briefly reaches boundary 1.

- During spark off time

$$K\frac{\partial T}{\partial y} = h_c(T - T_\infty) \quad \text{.....(3)}$$

- During spark on time:

$$K\frac{\partial T}{\partial y} = \begin{cases} q_x, & x \le x_s \\ h_c(T - T_\infty), & x \ge x_s \end{cases} \quad \text{.....(4)}$$

$$q_x = \frac{4.45FVI}{\pi R^2} e^{-3(x/x_s)^2} \quad \text{.....(5)}$$

Heat flux is assumed to be zero at boundary 2 because it is the axis of symmetry and there is no net heat gain or loss from this region when t>0. Boundary 3 and 4 are assumed to be insulated as these are far away, q_x is the amount of heat flux entering the workpiece, R is the radius of the spark (or plasma channel), h_c is the heat transfer coefficient, T_∞ is room temperature(298K).

In addition, the model is based on following assumptions

- A single spark is the focus of the created model.
- The volume of the removed material is far lesser than the volume of the workpiece,

Table 1
Mechanical property of the workpiece material.

Mechanical Property of SS304 Steel				
	Temperature (K)	**Thermal conductivity (W/mK)**	**Specific heat (J/kgK)**	**Density (kg/m³)**
1	298	14.9	502.5	8020
2	348	15.6	512.5	7995
3	373	16	517.5	7982
4	473	17.5	537.4	7932
5	573	18.9	557.3	7882
6	673	20.4	577.2	7832
7	973	24.7	636.8	7682
8	1473	31.5	735.9	7431
9	1644	32.4	769.6	7346

Table 2
Input combination for parametric analysis.

Input Combination			
S.N.	**Curent (A)**	**Voltage (V)**	**T_{on} (µs)**
1	10	30	100
2	30	30	100
3	50	30	100
4	50	30	50
5	50	30	25

hence the workpiece is thought of as a semi-infinite body.

- The thermal effects of subsequent sparks on one another are disregarded.
- Spark gap has little impact on discharge characteristics.
- The heat source is assumed to have Gaussian heat flow.
- During the analysis, phase changes are ignored.
- Each discharge causes a crater to form on the workpiece, which is considered to have circular parabolic geometry.
- After each spark, the recast layer is placed again in the crater, and this is regarded as uniform.
- After each spark, a recast layer lying outside the crater is redeposited on the workpiece is neglected.

It is found that the discharge column radius or plasma channel radius depends on the pulse on-time as well as the discharge current. As a result, the widely accepted Ikai and Hashigushi plasma channel radius equation has been applied (Ikai & Hashigushi, 1995).

$$R = (2.04exp - 3)I^{0.43}{t_{on}}^{0.44} \quad \text{.....(6)}$$

For each transient heat transfer study, the governing equation (Eq. 1) with given boundary conditions will be solved using the finite element method (FEM) to forecast the temperature distribution. For the analysis, a 2-D continuum of 120x100 mm is taken into account. For analysis, a two-dimensional, four-node quadrilateral element with a 1mm element is used. Materials with nonlinear characteristics, i.e. temperature-dependent thermal conductivity was used. The work is extended for Wire EDM with the various parameters after modelling, as shown in the table.

2.1. Model implementation

The numerical model was implemented using the analytical programme ABAQUS. The simulation is run using cathode as work material of stainless steel 304. Table 1 shows how the thermo-physical characteristics of SS304 change with temperature, including thermal conductivity, density and specific heat. These values are calculated using the following formulae provided in a referred work (Velencia & Quested, 2008).

$$K_t = \begin{cases} 10.33 + 15.4 * 10^{-3}T - 7 * 10^{-7}T^2 \\ \text{for } 298\text{K} \le T \le 1633\text{K} \\ 355.93 - 196.8 * 10^{-3}T \\ \text{for } 1644\text{K} \le T \le 1672\text{K} \\ 6.6 + 12.14 * 10^{-3}T \\ \text{for } T \ge 1793K \end{cases} \quad \text{....(7)}$$

$$C_p = 443 + 0.2T - 8 * 10^{-7}T^2 \quad \text{for } 298K \le T \le 1727K \quad \text{.....(8)}$$

$$\rho = \begin{cases} 8020 - 50.1 * 10^{-2}(T - 298) \\ \text{for } 298\text{K} \le \text{T} \le 1727K \\ 6900 - 80.0 * 10^{-2}(T - T_m) \\ \text{for T} \ge 1727\text{K} \end{cases} \quad \text{.....(9)}$$

Other considerations are: Liquidus temperature-1727k, Solidus temperature 1673k, Latent heat – 247000 (Govindan et al., 2013).

3. Results and Discussion

A parametric analysis is carried out to investigate how various operating parameters affect the

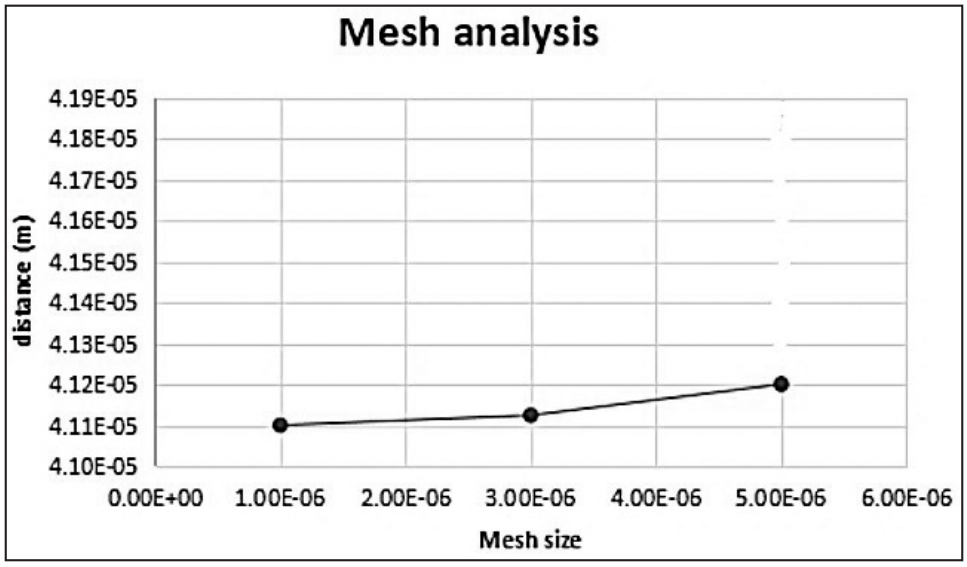

Fig. 2. Mesh sensitive analysis w.r.t. temperature profile.

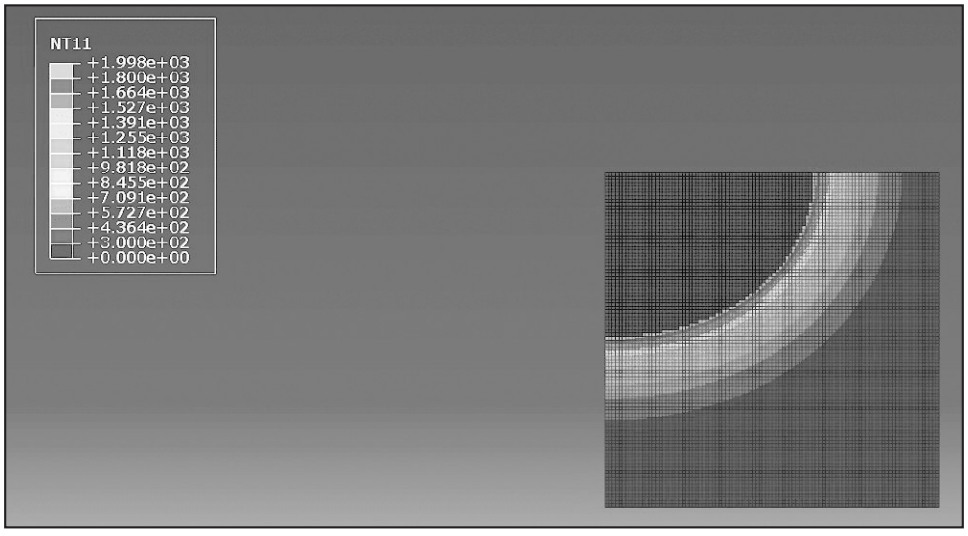

Fig. 3. Temperature profile at I-10A and T_{on}- 100 µs.

simulated temperature profile. Several FE simulations are run based on the parameter combinations given in Table 2.

3.1. Mesh sensitivity analysis

The chosen mesh size is of 1µm as the length of HAZ region along the depth with respect to duration of the spark i.e. T_{on} and T_{off} and changing mesh size do not show any large variation as shown in fig 2.

3.2. Effect of current

To analyse the effect of current, current value was is varied keeping the T_{on} constant and temperature profile is duly noted, seeing the heat penetration depth. Element with temperature greater than liquidous temperature is eliminated. In figures 3 and 4 it is observed that the material removed increases as the input current increases also leading to increase in spark radius but the depth of heat penetration is constant as interaction time is constant.

The maximum distance of heat penetration (HAZ region) along both axes is shown in Fig 5. As the current increases, the spark radius increases, hence much larger heat penetration along the horizontal direction. As the area increases for point of application of energy hence maximum energy penetrated along the depth is same.

3.3. Effect of on time (T_{on})

The effect of changing the T_{on} keeping the input current is observed in this analysis. As per the parameter mentioned in table 2. Temperature

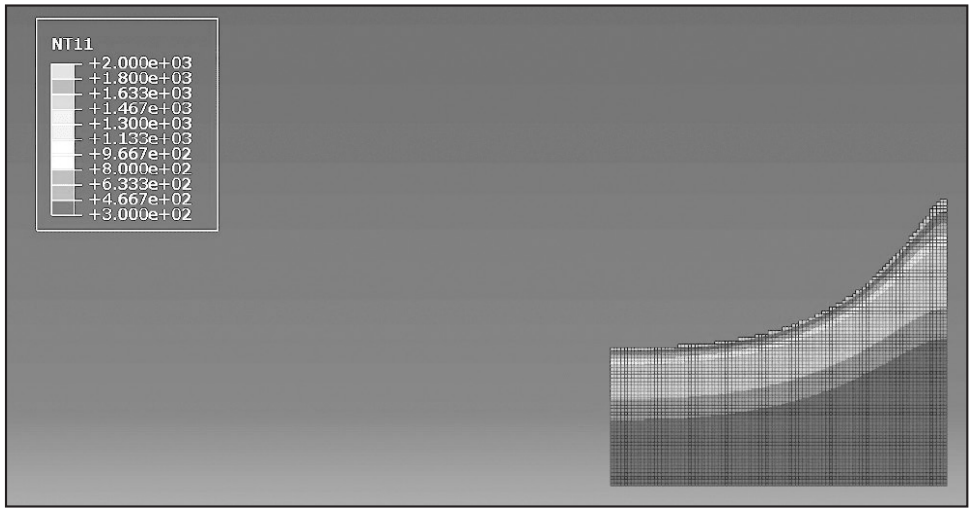

Fig. 4. Temperature profile at I-30A and T_{on}- 100 µs.

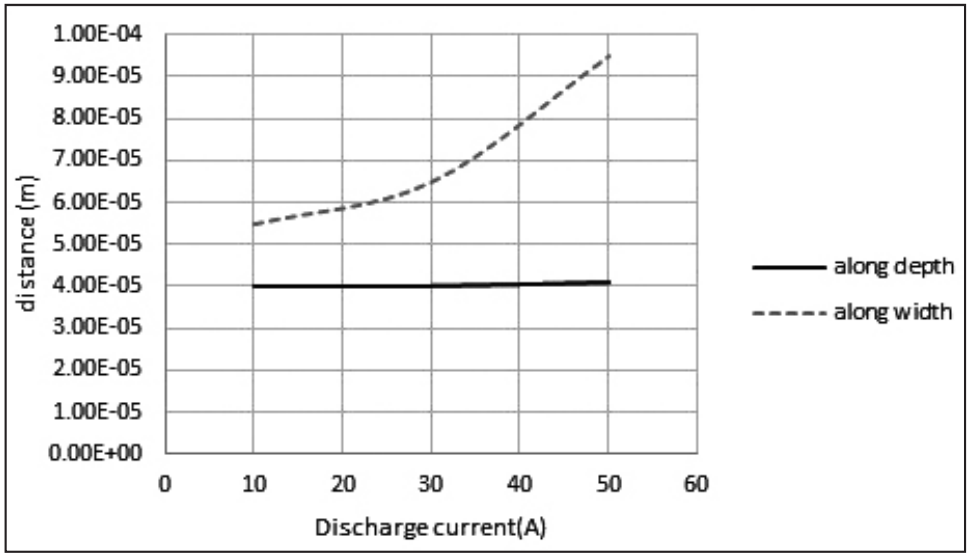

Fig. 5. Max distance of heat penetration along the axis.

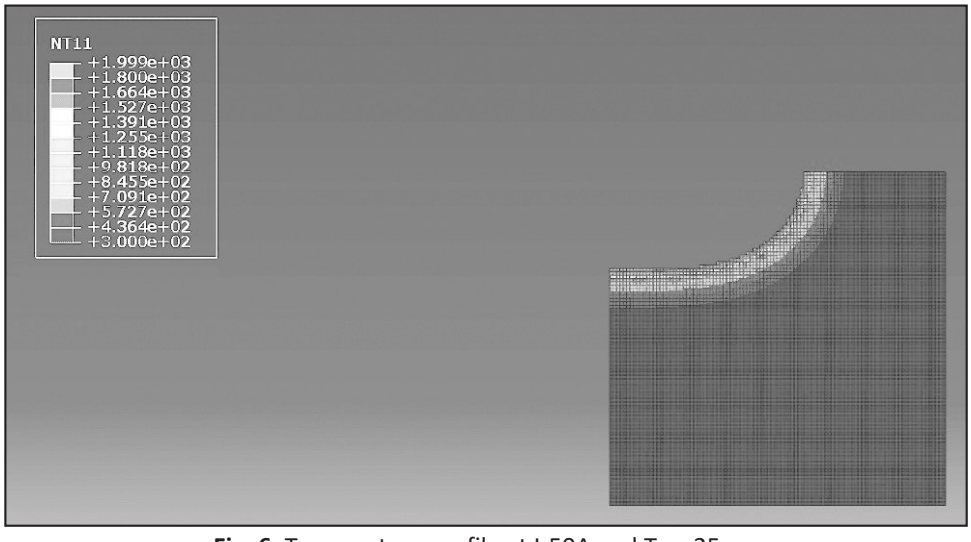

Fig. 6. Temperature profile at I-50A and T_{on} - 25 µs.

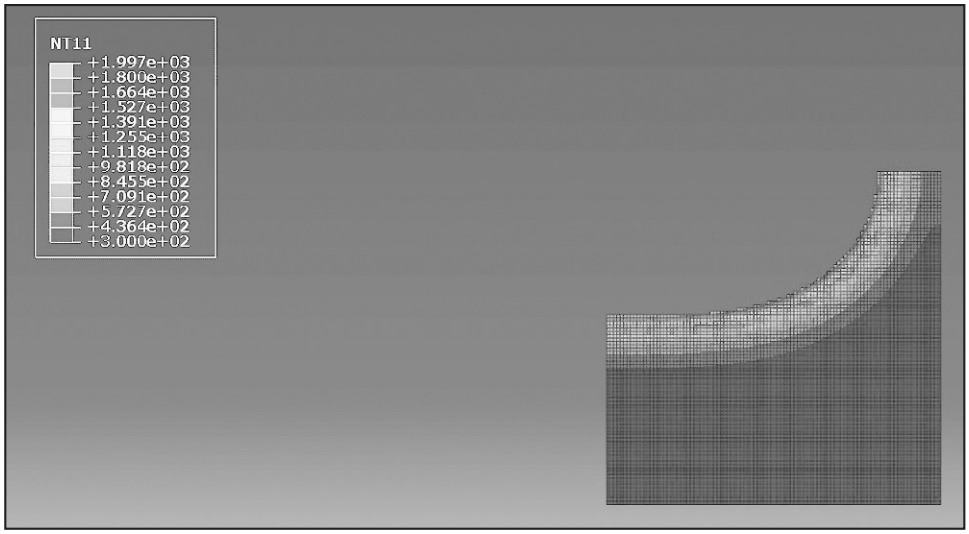

Fig. 7. Temperature profile at I-50A and T_{on} - 50 µs.

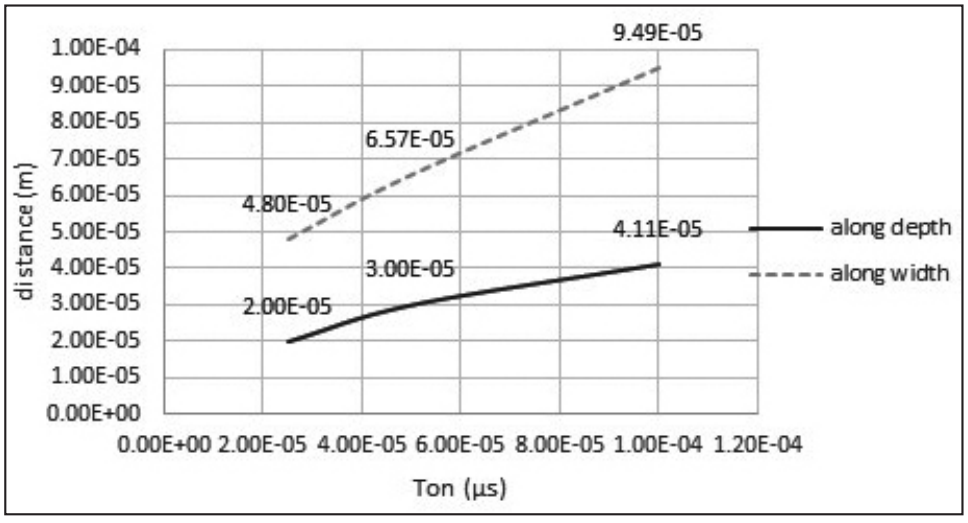

Fig. 8. Max distance of heat penetration along the axis leading to material removal and HAZ in the workpiece.

profile is studied and the distance of heat penetration in form of material removed duly noted showing the HAZ area of the process on the workpiece.

The temperature profile plot in fig. 6 and 7 shows the effect of T_{on} on the temperature profile of the EDM process. It can be concluded that as the Ton increases the Heat affected zone increases because spark radius increases and interaction time of the heat load increases. Its observed as the interaction time increases which lead to increase temperature variation along the depth also heat intensity increases as Ton increases. Since discharge current and discharge voltage are kept constant throughout all of these simulations, the input discharge power remains constant. However, as the pulse on-time grows, the plasma channel radius and the amount of time the cathode is exposed to the discharge power also do. As the pulse on-time grows, a bigger region becomes heated as a result higher HAZ zone is observed in the temperature profile.

Fig. 8. shows the maximum distance penetration of heat in the heat affected zone along the axis with respect to the above parameter analysis. This analysis shows that the Current and Ton are an important EDM process parameter. In fig 5 Minimum heat penetration in HAZ region is observed at current of 10A. This is due to the fact that at low currents, a sufficiently strong pulse is not produced to produce enough heat to enter the cathode body leading to which the heat affected zone is minimum. It has also been seen that the depth of temperature variation is constant as interaction time is constant.

In Fig 8, the heat flux is supplied for a longer time as the pulse on time lengthens, allowing the heat to more effectively pierce the cathode body, increasing the temperature affected zone.

4. Conclusion

The above model provides conclusive relation of temperature distribution of the Electro discharge Machining process. Conclusion to the FEM analysis are as:

- Increase in pulse on time lead to increase in heat affected zone along the depth. 50% increase in Ton gives almost 33% increase in heat affected zone along the depth and almost 28 % increase along the width.
- Increasing the pulse current shows very low variation of heat penetration along the depth and high heat penetration along the width as spark radius increases.
- Short pulse duration has lower heat-affected zone compared to high pulse duration hence low material removal.

References

DiBitonto, D. D., Eubank, P. T., Patel, M. R., & Barrufet, M. A. (1989). Theoretical models of the electrical discharge machining process. I. A simple cathode erosion model. *Journal of Applied Physics, 66*(9), 4095-4103.

Govindan, P., Gupta, A., Joshi, S. S., Malshe, A., & Rajurkar, K. P. (2013). Single-spark analysis of removal phenomenon in magnetic field assisted dry EDM. *Journal of Materials Processing Technology, 213*(7), 1048-1058.

Hargrove, S. K., & Ding, D. (2006). Determining cutting parameters in wire EDM based on workpiece surface temperature distribution. *The International Journal of Advanced Manufacturing Technology, 34*(3-4), 295-299.

Ikai, T., & Hashigushi, K. (1995). Heat input for crater formation in EDM. *Proceedings of the International Symposium for Electro-Machining-ISEM XI*, EPFL, 163-170.

Joshi, S. N., & Pande, S. S. (2010). Thermo-physical modeling of die-sinking EDM process. *Journal of Manufacturing Processes, 12*(1), 45-56.

Kalajahi, M. H., Rash Ahmadi, S., & Oliaei, S. N. B. (2013). Experimental and finite element analysis of EDM process and investigation of material removal rate by response surface methodology. *The International Journal of Advanced Manufacturing Technology, 69*(1-4), 687-704.

Schumacher, B. M. (2004). After 60 years of EDM the discharge process remains still disputed. *Journal of Materials Processing Technology, 149,* (1-3), 376-381.

Valencia, J. J., & Quested, P. N. (2008). Thermophysical Properties. *Casting*, 468-481.

Yadav, V., Jain, V. K., & Dixit, P. M. (2002). Thermal stresses due to electrical discharge machining. *International Journal of Machine Tools and Manufacture, 42*(8), 877-888.

S. C. Sonthalia is a Dual Degree candidate in the Department of Mechanical Sciences at IIT Bhubaneswar. His area of interest included Micro-machining, Surface Engineering. His research areas are investigating surface modification techniques using various Non-Convectional Processes such as W-EDM, Laser machining, and Chemical Machining.

Dr. Gaurav Bartarya did his Master's and Ph.D from Indian Institute of Technology Kanpur. Before that, he completed his B.Tech from GBPUAT Pantnagar. He is currently working as Assistant Professor at Indian Institute of Technology Bhubaneswar, India. His preliminary area of interest is conventional machining of hard materials. He has worked extensively on surface integrity issues in hard turning of steel, concerned with process performance modelling and surface integrity issues like white layer, tensile residual stresses etc. prevailing during hard turning. He also works in advance machining processes, incremental forming and reverse engineering.
(E-mail: bartarya@iitbbs.ac.in)

Dr. S. Mullick is currently working as Assistant Professor in School of Mechanical Sciences of IIT Bhubaneswar, India since July, 2017. He completed his M.Tech (2011) and Ph.D (2016) from the Mechanical Engineering Department, IIT Kharagpur, India. He has worked extensively in the field of laser material processing, like conventional and underwater laser cutting, laser grooving, paint removal under wet and dry conditions, etc. His current interest is the laser-based additive manufacturing of MMC, online monitoring of molten pool thermal history during laser-based deposition process, ultrasonic vibration assisted laser deposition, development and experimental investigation on water-assisted wet laser processing, like welding, surface treatment. He has co-authored several journal and conference papers in related research areas.
(E-mail: suvradip@iitbbs.ac.in)